OFFICE OF NAVAL RESEARCH

Contract N00014-82-0280

Task No. NR413EOOl

TECHNICAL REPORT NO. 53

Electron Energy Loss Investigation of Hole-plasmon Excitation Following the in situ Doping of Si(111) by Boron

by

P.J. Chen, J.E. Rowe, and J.T. Yates, Jr.

Submitted To

Phys. Rev. B

Surface Science Center
Department of Chemistry
University of Pittsburgh
Pittsburgh, PA 15260

September 28, 1992

REPORT DOCUMENTATION PAGE

READ INSTRUCTIONS BEFORE COMPLETING FORM

1. REPORT NUMBER: 53	2. GOVT ACCESSION NO.
3. RECIPIENT'S CATALOG NUMBER	
4. TITLE (and Subtitle): Electron Energy Loss Investigation of Hole-plasmon Excitation Following the in situ Doping of Si(111) by Boron	5. TYPE OF REPORT & PERIOD COVERED: Preprint
	6. PERFORMING ORG. REPORT NUMBER
7. AUTHOR(s): P.J. Chen, J.E. Rowe and J.T. Yates, Jr.	8. CONTRACT OR GRANT NUMBER(s)
9. PERFORMING ORGANIZATION NAME AND ADDRESS: Surface Science Center, Department of Chemistry, University of Pittsburgh, Pittsburgh, PA 15260	10. PROGRAM ELEMENT, PROJECT, TASK AREA & WORK UNIT NUMBERS
11. CONTROLLING OFFICE NAME AND ADDRESS	12. REPORT DATE: September 28, 1992
	13. NUMBER OF PAGES
14. MONITORING AGENCY NAME & ADDRESS (if different from Controlling Office)	15. SECURITY CLASS. (of this report): Unclassified
	15a. DECLASSIFICATION/DOWNGRADING SCHEDULE

16. DISTRIBUTION STATEMENT (of this Report)

17. DISTRIBUTION STATEMENT (of the abstract entered in Block 20, if different from Report)

18. SUPPLEMENTARY NOTES

19. KEY WORDS (Continue on reverse side if necessary and identify by block number)

Boron, decaborane, electron energy loss spectroscopy
Silicon, Surface plasmon
Si(111), diffusion

20. ABSTRACT

High resolution electron energy loss spectroscopy (HREELS) measurements have been performed on Si(111) surfaces heavily p-doped by the decomposition of adsorbed decaborane. After thermal decomposition of the decaborane to produce B atoms on the surface, the low energy electron diffraction pattern shows a $(\sqrt{3}\times\sqrt{3})R30°$ periodicity due to the presence of 1/3 monolayer of boron in the second complete layer. The HREELS data exhibit two strong features: (1) the B-Si dipole mode at 96 meV and (2) a broad surface plasmon mode is observed at ~100 meV loss energy due to the free carriers in the region below the B-reconstructed surface layer. We have investigated the electron energy dependence of the surface plasmon mode in order to determine the feasibility of using HREELS to determine the depth profile of the free carriers due to B diffusion into the region 100-1000 Å below the surface. Unexpectedly, we find that kinematic factors play an important role in the electron energy range used, 15 - 28 eV, and thus limit the degree of quantitative information that can be obtained about the carrier depth profile from HREELS data.

DD FORM 1 JAN 73

E (When Data Entered)

Submitted to: Phys. Rev. B
Date: September 28, 1992

Electron Energy Loss Investigation of Hole-plasmon Excitation Following the *in situ* Doping of Si(111) by Boron

P. J. Chen
Department of Physics, University of Pittsburgh
Pittsburgh, PA 15260

J. E. Rowe
AT&T Bell Laboratories
Murray Hill, NJ 07974

and

J. T. Yates, Jr.
Surface Science Center
Department of Chemistry, University of Pittsburgh
Pittsburgh, PA 15260

PACS Numbers: 61.70.Sk, 68.55.Ln, 73.20.Mf, 79.20.-m

ABSTRACT

High resolution electron energy loss spectroscopy (HREELS) measurements have been performed on Si(111) surfaces heavily p-doped by the decomposition of adsorbed decaborane. After thermal decomposition of the decaborane to produce B atoms on the surface, the low energy electron diffraction pattern shows a $(\sqrt{3}x\sqrt{3})R30°$ periodicity due to the presence of 1/3 monolayer of boron in the second complete layer. The HREELS data exhibit two strong features: (1) the B-Si dipole mode at 96 meV and (2) a broad surface plasmon mode is observed at ~100 meV loss energy due to the free carriers in the region below the B-reconstructed surface layer. We have investigated the electron energy dependence of the surface plasmon mode in order to determine the feasibility of using HREELS to determine the depth profile of the free carriers due to B diffusion into the region 100-1000 Å below the surface. Unexpectedly, we find that kinematic factors play an important role in the electron energy range used, 1.5 - 28 eV, and thus limit the degree of quantitative information that can be obtained about the carrier depth profile from HREELS data.

1. INTRODUCTION

An important parameter for the understanding of the space-charge region near the surface of a semiconductor is the doping density and the doping concentration profile or dependence on depth. Although sputter-profile analysis such as Secondary Ion Mass Spectrometry (SIMS) can give the atomic concentration profile, direct measurements of the carrier concentration profile usually require contacts and/or interface formation with metals or other semiconductors. It is well known that one can probe the carrier density through the low energy free-carrier plasmon excitation using high resolution electron energy loss spetroscopy (HREELS) [1-5] since the probing depth can extend to ~3000 Å depending upon the excitation energy and the energy of the incident electrons. In this paper we report experiments using HREELS to probe the carrier-hole plasmon exciton in the space-charge region 100-1000 Å below the surface of Si(111). We have explored the possibility of measuring the doping profile that occurs after *in situ* boron doping of the Si(111) surface by thermal diffusion of surface boron atoms produced by thermal decomposition of adsorbed decaborane molecules. An effective carrier-hole concentration on the order of $\sim 10^{19}$ cm^{-3} has been deduced from the HREELS measurements for monolayer-level boron initially deposited on the surface. The surface hole-plasmon is highly damped due to the low mobility of carrier holes at such high concentrations and due

to the strong intravalence band transitions resulting from the small spin-orbit splitting of the valence band for Si (35 meV). Under these conditions, kinematic effects in HREELS have to be taken into account in order to give a quantitative description of the electron energy loss features. Dipole scattering theory in conjunction with the long-wavelength Thomas-Fermi dielectric function gives an adequate description of the electron energy-loss features. However, the ability for HREELS to probe different regions of the space-charge layer below the surface is limited by kinematic and finite spectrometer acceptance angle effects, especially at low incident electron energies.

2. EXPERIMENTAL

The HREELS measurements were performed in a UHV system with a typical base pressure of $1x10^{-10}$ mbar. The HREELS measurements were carried out in the specular scattering geometry with a 60° incident angle at electron energies 1.5 - 28 eV. The HREELS data were recorded in a pulse-counting mode with an energy increment of 0.6 meV and are presented without any post-acquisition treatment. The boron deposition was carried out by thermally decomposing decaborane molecules [6,7] initially adsorbed on Si(111). Subsequent annealing at 1200 - 1300 K promoted boron diffusion into the bulk of Si(111). The details of this study are reported elsewhere [7].

The surface structure of the B-modified $(\sqrt{3}x\sqrt{3})R30°$ Si(111) surface is shown in Figure 1a. The surface Si atoms occupy the T_4 adatom sites to form an ordered $(\sqrt{3}x\sqrt{3})R30°$ superstructure on top of the (1x1) bulk-terminated Si lattice. The B atoms occupy the substitutional, subsurface S_5 sites in the first Si bilayer directly below the surface Si adatoms [8-10]. The nominal subsurface B concentration is 0.33 per (1x1) unit cell or 1/3 monolayer.

The existence of an extensive body of knowledge on boron diffusion in Si allows a reliable estimation of the B diffusion length in Si(111) under our experimental conditions. For the B concentration of interest here, the diffusion is in the extrinsic regime, i.e., the diffusion coefficient is concentration dependent. Based on the annealing temperature and time, an empirical diffusion law based on the extrinsic model [11] estimates a B diffusion length of 10^3-10^4 Å. This distance has been verified by secondary ion mass spectroscopy (SIMS) depth profile measurements performed separately *ex situ* on our doped Si(111) crystals. Since the typical characteristic wavevector transfer involved in dipole scattering is ~10^{-2} Å^{-1} in the present HREELS [1], the amplitude of the excited plasma wave decays

exponentially into the bulk on a length scale significantly smaller than the B diffusion depth. Thus, the B-doped region below the Si(111) surface is essentially bulk-like in terms of its dynamic response to the low energy electrons. This gives rise to the electron energy loss features to be discussed below.

3. RESULTS

3.1 HREELS Observation of the B-Si Vibrational Mode and Surface Hole-plasmon Excitation

After boron deposition and annealing to form the ordered $(\sqrt{3}x\sqrt{3})R30°$ surface, a typical HREEL spectrum taken at 100 K from the Si(111)-B$(\sqrt{3}x\sqrt{3})R30°$ surface is shown in Figure 1b. There are two very distinct energy loss features in the spectrum. The free-carrier surface plasmon excitation in the highly B-doped region below the surface gives rise to a broad energy-loss feature centered at ω_{pp}. Superimposed on this background is a sharp loss peak at 96 meV which belongs to a B-Si vibrational mode (optical phonon) localized in the surface region. In an earlier work, Rowe and coworkers [12] have characterized this mode as a breathing motion of B in the S_5 lattice site in Si.

Since the free-carrier plasmon frequency is proportional to $n^{1/2}$ (n = carrier density), varying the doping level in Si is expected to have a direct effect on the observed loss peak position, ω_{pp}, due to the surface plasmon. This characteristic is verified qualitatively in the HREEL spectra (Figure 2) taken at a constant electron energy, E_0=6.1 eV, on selectively B-doped Si(111) with increasing amounts of boron as judged by the Auger intensity ratios. The inset of Figure 2 shows the expected dependence on boron density (determined by Auger intensity) for all but the highest exposure. It is also clear that the frequency of the localized B-Si vibrational mode remains unaffected by the variation in n. Since this vibration is a true surface mode originating from the vibration of substitutional B atoms against the surrounding Si neighbors, the vibrational amplitudes are localized in the top two or three atomic layers. Therefore, unlike the optical phonons (the Fuchs-Kleiwer modes) in bulk polar semiconductors such as GaAs [13], this localized B-Si optical phonon is not expected to couple to the carrier surface plasmon.

3.2 Electron Energy Dependence of Hole-plasmon Loss

Figure 3 shows a series of HREEL spectra taken at 100 K from a well-ordered $(\sqrt{3}x\sqrt{3})R30°$ surface at various primary electron energies, E_0. The intensity of the localized B-Si vibration decreases monotonically with increasing E_0. This behavior is consistent with the dipole scattering mechanism which predicts an E_0^{-1} dependence in the loss intensity [1]. Another prominant characteristic observed from these HREEL spectra is that the loss feature due to surface plasmon excitation experiences a pronounced upshift in peak energy with increasing E_0. Since the peak-position shift exhibited in the spectra appears to be similar to what was observed when the boron concentration was changed, it might be tempting to interpret this phenomenon in the context of a changing carrier concentration, n, as the effective probing depth of HREELS (to be defined later) varies with E_0. However, it has been recently demonstrated on GaAs [14,15] that the kinematic factor in dipole scattering plays an important role for surface hole-plasmon excitation. Thus any quantitative interpretation of the E_0-dependent spectra obtained here has to take this into account. In order to fully address these physical issues contained in our experimental measurements, we next present a model dielectric function analysis of the electron energy loss cross section based on the well-accepted dipole scattering mechanism. This is followed by a comparison of numerically simulated energy loss spectra with experimental measurements.

4. Theoretical Analysis

4.1. Model Dielectric Function

We adopt a long-wavelength, local-dielectric-response theory upon which to base our model calculation and consider only a constant carrier concentration, n, for simplicity. The dielectric response of the free-carrier holes is assumed to be described by the frequency and wavevector dependent Thomas-Fermi dielectric function, ε_{TF}:

$$\varepsilon_{TF}(\omega,\boldsymbol{k}) = \varepsilon_\infty - \frac{4\pi e^2 n}{m[\omega^2 + i\omega\Gamma - D(\boldsymbol{k})]} = \varepsilon_\infty - \frac{\omega_p}{\omega^2 + i\omega\Gamma - D(\boldsymbol{k})} \qquad (1)$$

with $D(\boldsymbol{k}) = \frac{3}{5}k^2 v_F^{\,2}$, where v_F is the Fermi velocity, ω_p is the bulk plasma frequency and ε_∞ is the high-frequency dielectric constant. The damping factor, Γ, is directly related to the carrier-hole mobility, μ_h, by

$$\Gamma = \frac{e}{m_h \mu_h} \tag{2}$$

where e is the electronic charge. The effective mass of the carrier-holes is taken from the contribution of both light and heavy holes in the form [14]

$$\frac{1}{m_h} = \frac{n_{lh}}{m_{lh}} + \frac{n_{hh}}{m_{hh}} \tag{3}$$

where n_{lh} and n_{hh} are the concentration of light and heavy holes in Si.

In the limit of long-wavelength and zero-damping, the surface plasmon frequency, ω_{sp}, is defined as

$$\omega_{sp} = \left(\frac{4\pi e^2 n}{m(\varepsilon_\infty + 1)} \right)^{1/2} = \frac{\omega_p}{\sqrt{\varepsilon_\infty + 1}} \tag{4}$$

which relates ω_{sp} directly to $n^{1/2}$.

This choice of dielectric function is based on the following physical considerations for our system: (i) the k-range involved in our near-specular HREELS measurements is at least one order of magnitude smaller than the Fermi wavevector, k_F, at the carrier density ($\sim 10^{19}$ cm^{-3}) under study. Thus the experiments essentially explore the dielectric response of the system in the long-wavelength limit; (ii) at such a high doping level, the Thomas-Fermi screening length is very short (a few Å) compared to the depth ($\sim 10^3$ Å) of the free-carrier space-charge region. Thus a physical condition exists to apply the local response formalism. In addition, a quantitative comparison between the local-response and a nonlocal theory [16,17] under accumulation layer conditions indicates a very promising agreement between the two at long wavelengths, the important region for HREELS.

4.2 Dipole Scattering Mechanism and Kinematic Effects

In the dipole scattering theory which describes the electron energy loss process due to collective excitations at a solid surface, the spectral intensity $I(\omega)$ or differential cross section (normalized to elastic intensity) is represented in a 2-D momentum space integral [1,3] which contains a product term of the kinematic factor and the loss-function

Im[-1/(ε+1)] integrated over the parallel momentum transfer range, Q_C, defined by the spectrometer acceptance angle, ϑ_C.

$$I(\omega) = \frac{4e^2 v_\perp^{\ 2}}{\pi^2 \hbar^2}\left(\frac{k_S}{k_I}\right)\int_{Q<Q_C} \frac{Q\,d^2Q}{[v_\perp^{\ 2}Q^2 + (\omega - v_\parallel \cdot Q)^2]^2}[1 + n(\omega)]\mathrm{Im}\left[\frac{-1}{\varepsilon(\omega, Q)+1}\right] \qquad (5)$$

where k_I and k_S are the wavevectors of the incident and scattered electron respectively and $n(\omega)$ is the Bose-Einstein factor. Inside the k-space integral, the kinematic factor acts as a weighing function on the loss-function, Im[-1/(ε+1)], at each parallel momentum transfer, Q. If we are in the parameter regime of small damping where the loss-function consists of sharp peaks with narrow widths (such as the optical phonons in an ionic crystal), varying the kinematic factor only modulates the intensities of the energy loss peaks in the final outcome of the k-integral in $I(\omega)$ (assuming small dispersion of ε). The loss peak positions essentially coincide with the poles in Im[-1/(ε+1)]. On the other hand, if the loss-function contains a broad frequency response due to large damping, kinematic effects will then become important in determining the peak position in the differential cross section, $I(\omega)$. This type of loss-function Im[-1/(ε+1)] is encountered in the current study of surface hole-plasmon excitation in the heavily B-doped Si(111). Again, under the conditions of negligible dispersion with k, the energy position of the observed loss peak in $I(\omega)$ differs from the peak position of Im[-1/(ε+1)] by virtue of the strong ω-dependence of the kinematic factor. At the doping levels currently achieved, the damping width of the hole plasmon, Γ, becomes comparable to the surface plasmon frequency, ω_{sp}, due to strong scattering of carrier-holes by the ionized dopants. Under this circumstance, the observed loss peak position, ω_{pp}, can no longer be simply equated to ω_{sp} as defined by eqn. (4), and a full evaluation of $I(\omega)$ is generally necessary in order to obtain ω_{sp}, n_h and Γ from the measured energy loss spectrum.

Another well-known aspect of the kinematic effect in dipole scattering is the selectivity in Q, the parallel momentum transfer, with varying E_0. At a given E_0 and for a given energy loss, $\hbar\omega$, the kinematic factor (or the dipole lobe) peaks sharply at a particular wave vector $Q \sim (\hbar\omega/2E_0)k_0$. Consequently, a region of the space-charge layer defined by an effective sampling depth, $d_{eff} \sim Q^{-1}$, is selectively probed by the low energy electron [1]. It has been suggested [1,3,4,17] that this property can be utilized as a potentially meaningful experimental tool to probe the dynamics of a non-uniform space-charge layer in a depth-resolved fashion, especially in the near surface region (10^2 - 10^3 Å). However, by varying the incident electron energy, E_0, not only the sampling depth,

d_{eff}, is changed, but the kinematic factor is also effectively changed as well. Under the conditon of large damping, the kinematic effects of varying E_0 should also be considered in interpreting the E_0-dependent plasmon loss spectra. This will be presented below with a numerical evaluation of eqn.(5) using parameters best representing the experimental conditions.

5. COMPARISON BETWEEN THEORY AND EXPERIMENT

The model calculation incorporating both the dipole scattering kinematics and the model dielectric function is carried out numerically by assuming a circular spectrometer aperture and a fixed value of ϑ_C=2.5°. This will provide the basis for a more quantitative consideration of the experimental data and understanding of the physics contained in the HREELS measurements.

As a start, we apply the formalism outlined above to generate a theoretical energy loss spectrum. The carrier density, n_h, and the damping factor, Γ, are used essentially as fitting parameters to the experimental spectrum. Figure 4 shows the comparison between the measured data (points) and the fit (solid line). The overall quantitative agreement between theory and experiment is good. It should be pointed out that the theoretical curve is not sensitive to ϑ_C because at E_0=24 eV, the scattered electron angular distribution is very narrow and the dipole lobe peaks at $\vartheta < 0.2°$ away from specular direction. Virtually all the scattered electron intensity is collected by the spectrometer aperture, ϑ_C =2.5°, used in the calculation. The 'best fit' yields n_h=2.8x10^{19} cm^{-3} and Γ= 74 meV, which corresponds to a ω_{sp}=102 meV. We treat the carrier density n_h determined in this fashion as an "effective" carrier density which is an average over the distance of the effective electron sampling depth, d_{eff}, defined earlier. At E_0=24 eV, this yields $d_{eff} \approx$ 440 Å at the observed plasmon peak energy. The damping term, Γ, is related to the carrier-hole mobility, μ_h, through eqn. (2) given in Section 4.1, from which a value μ_h= 54 cm^2/V sec is obtained through the fitting. This value agrees well with the reported hole mobility in heavily B-doped Si [18]. Also plotted in Figure 4 (dashed curve) is the k-integrated loss function, Im[-1/(ε+1)], which is used to illustrate the effect in the absence of the kinematic factor. Its behavior shows that in the k-range explored in HREELS, dispersion in ε_{TF} has only a negligibly small effect on the energy-loss peak position. The dominating factor for shifting the peak position away from that of Im[-1/(ε+1)] is the strong ω-dependence of the kinematic factor. It is clear from Figure 4 that when $\omega_{sp} \sim \Gamma$, the full spectrum $I(\omega)$ and the k-integrated loss function peak at different ω values.

Incidentally, neither peak position corresponds to the surface plasmon energy, ω_{sp}, defined by eqn. (4). For precisely this reason, the determination of n_h from the observed loss peak position is no longer straightforward. A simplified relation linking the observed loss peak position, ω_{pp}, and the surface plasmon frequency, ω_{sp}, has been given by Meng et al. [14] under the approximation of a $1/\omega$-like behavior of the kinematic factor.

Next, we use the same fitting parameters to generate a set of simulated spectra with varying E_0. These results are shown in Figure 5. Varying the electron energy, E_0, as noted before, effectively varies the effective electron probing depth, d_{eff}, and the kinematic factor. It can be seen from the calculated energy loss spectra that the major effect is a modulation to the loss intensities. For electron energy $E_0 > 10$ eV, the loss peak position remains essentially unchanged. Below this electron energy, a widening dipole lobe moving away from the specular direction results in an intensity cut-off on the high energy-loss side due to a finite spectrometer acceptance aperture, ϑ_c. This high energy-loss cut-off causes the overall weight of the energy loss features to shift toward lower energy-loss side. Numerical calculations with two different ϑ_c values clearly indicate this effect as shown in Figure 5. Even with a constant carrier density n_h, such kinematic effects are strong under the condition of large damping in the loss function, $\mathrm{Im}[-1/(\varepsilon+1)]$.

Comparison between the experimental data (Figure 3) and the theoretical simulation in Figure 5 shows reasonable qualitative agreement. The general behavior of the loss intensities exhibited in the experimental spectra are fairly well reproduced in the simulation. However, the experimental spectra appear to show a much more pronounced peak shift than the simple uniform model dielectric function would predict with a physically reasonable spectrometer angular acceptance. Such a downshift in plasmon loss peak energy with decreasing E_0 can be clearly seen by inspecting the measured and simulated spectra in the electron energy range 6 - 28 eV where the spectrometer acceptance angle effect is minimized. This suggests that there is also a significant contribution from a non-uniform carrier concentration profile (such as a depletion layer) in the near surface region (100 - 400 Å) that enters into the measured energy loss spectra. But the full analysis is difficult due to the small spectrometer acceptance aperture cut-off effect. This situation exists for most HREEL spectrometers in operation today.

The suggestion of a non-uniform carrier concentration over the HREELS probing depth (100 - 400 Å) is further substantiated by *ex situ* dynamic SIMS analysis performed on this Si(111) crystal. The sputter-profile measurement verifies the existence of a boron

concentration gradient which is characterized by a sharp rise (about one order of magnitude) in boron concentration over the initial ~300 Å in depth [19]. This trend is in excellent agreement with the prediction of the HREELS analysis presented above.

The dependence of the effective electron probing depth, d_{eff}, on the incident electron energy has been discussed in the past. A number of studies (mostly on group III-V compound semiconductors) have been carried out [2-5, 13-15] under various bulk doping conditions. Our current results clearly suggest that in the limit of small damping (such as for the high-mobility free electrons in III-V semiconductors), it is feasible to utilize the depth-probing capability of HREELS to study the space-charge region near the surface of a semiconductor in a quantitative and, more importantly, non intrusive fashion. However, when the plasmon damping, Γ, becomes comparable to the surface plasmon frequency, ω_{sp}, kinematic effects in HREELS, as discussed above, will limit the extent of quantitative physical information that can be extracted from the observed energy loss spectra.

Finally, we briefly discuss the role of the ordered $(\sqrt{3}x\sqrt{3})R30°$ subsurface B layer which has been largely ignored in previous treatments. As a p-type dopant in bulk Si, B produce charge carriers (holes) in the Si valence band via thermal exitation of valence electrons into the B acceptor levels near the edge of Si valence band. However, we argue that based upon the unique surface electronic structure of the boron-modified Si(111), the ordered 1/3 ML B atoms are electrically inactive in terms of fulfilling their usual acceptor function. Because of the termination of the bulk crystal structure and the $(\sqrt{3}x\sqrt{3})R30°$ surface reconstruction, these subsurface B atoms no longer provide similar acceptor levels near the edge of the Si valence band as bulk dopant B atoms do. The B-induced band-gap surface states lie 1.3-1.8 eV above the valence band maximum (VBM) [20] and remain unoccupied at 100 K while the electron density originally associated with the surface Si adatoms redistributes toward the subsurface B, producing an occupied surface state below VBM. As a result, no charge carrier (hole) is produced in the bulk Si valence band by these specially-coordinated subsurface B atoms. In the frequency range of interest here, the dielectric response of this near surface layer only comes from the B-Si optical phonon plus the contributions from the ion cores.

6. SUMMARY AND CONCLUSIONS

We have used HREELS to explore the dielectric response in the near surface region of a highly B-doped Si(111) crystal. The main conclusions can be summarized as follows:

1. Following the thermal diffusion of boron in the Si(111), surface plasmon excitation due to the free-carrier holes has been observed by specular HREELS at 100 K in the electron energy range 1.5-28 eV. The hole-plasmon is highly damped due to the scattering of carriers by the ionized dopants and contributions from intravalence band transitions.
2. The dipole scattering theory combined with a Thomas-Fermi model dielectric function has been shown to provide a proper description of the electron energy loss cross section. Kinematic effects have to be taken into account in order to make a quantitative interpretation of experimental electron energy loss features and deduce the surface plasmon frequency, ω_{sp}.
3. Evidence for a non-uniform carrier concentration in the near surface region (<1000 Å) has been suggested by comparison of HREELS data and model calculations.
4. At very low electron energies (E_0 < 5 eV), the combination of strong damping and finite spectrometer acceptance angle cut-off complicates the quantitative interpretation of the experimental HREELS data.

ACKNOWLEDGEMENT

We thank Dr. L. Feldman of AT & T Bell Laboratories for carrying out nuclear activation analysis on our Si(111) crystals and Dr. L. C. Hopkins for making SIMS measurements. The experimental help of Mr. M. L. Colaianni is gratefully acknowledged. We acknowledge the financial support of this work by the Office of Naval Research.

References

[1] H. Ibach and D. L. Mills, "Electron Energy Loss Spectroscopy and Surface Vibrations", Academic Press, New York (1982), pg. 79-84.

[2] J. A. Stroscio and W. Ho, Phys. Rev. Lett. 54 (1985) 1573.

[3] L. H. Dubois, B. R. Zegarski and B. N. J. Persson, Phys. Rev. B35 (1987) 9128.

[4] Z. J. Gray-Graychowski, R. G. Egdell, B. A. Joyce, R. A. Stradling and K. Woodbridge, Surf. Sci. 186 (1987) 482.

[5] J. M. Seo, D. S. Black, P. H. Holloway and J. E. Rowe, J. Vac. Sci. Technol. A6 (1988) 1523.

[6] Ph. Avouris, I.-W. Lyo, F. Boszo and E. Kaxiras, J. Vac. Sci. Technol. A8 (1990) 3405.

[7] P. J. Chen, M. L. Colaianni and J. T. Yates, Jr., J. Appl. Phys., in press.

[8] R. L. Headrick, I. K. Robinson, E. Vlieg and L. C. Feldman, Phys. Rev. Lett. 63 (1989) 1253.

[9] P. Bedrossian, R. D. Mead, K. Mortensen, D. M. Chen, J. A. Golovchenko and D. Vanderbilt, Phys. Rev. Lett. 63 (1989) 1257.

[10] I.-W. Lyo, E. Kaxiras and Ph. Avouris, Phys. Rev. Lett. 63 (1989) 1261.

[11] S. M. Sze, "Semiconductor Devices", Wiley, New York (1985), pg.391.

[12] J. E. Rowe, R. A. Malic, E. E. Chaban, R. L. Headrick and L. C. Feldman, J. Electron Spect. Rel. Phenomn. 54/55 (1990) 1115.

[13] Y. Chen, S. Nannarone, J. Schaefer, J. C. Hermanson and G. J. Lapeyre, Phys. Rev. B39 (1989) 7653.

[14] Y. Meng, J. R. Anderson, J. C. Hermanson and G. J. Lapeyre, Phys. Rev. B44 (1991) 4040.

[15] Y. Meng, J. Anderson and G. J. Lapeyre, Phys. Rev. B45 (1992) 1500.

[16] B. Xu and J. C. Hermanson, Phys Rev. B40 (1989) 12539.

[17] D. H. Ehlers and D. L. Mills, Phys. Rev. B36 (1987) 1051.

[18] G. Masetti, M. Severi and S. Solmi, IEEE Trans. Electron Dev. 30 (1983) 764.

[19] J. E. Rowe, unpublished.

[20] E. Kaxiras, K. C. Pandey, F. J. Himpsel and R. Tromp, Phys. Rev. B41 (1990) 1262.

Figure Captions

Figure 1: (a) The structure of the Si(111)-B($\sqrt{3}$x$\sqrt{3}$)R30° surface with the ($\sqrt{3}$x$\sqrt{3}$)R30° unit cell outlined. The B atoms occupy the subsurface, substitutional S_5 sites in the first Si bilayer. (b) HREEL spectrum taken from a well-ordered Si(111)-B($\sqrt{3}$x$\sqrt{3}$)R30° surface at 100 K with a primary electron energy E_0=3.2 eV. The peak position corresponding to the surface hole-plasmon loss, ω_{pp}, is at 63 meV. The loss peak belonging to the localized B-Si optical phonon mode is at 96 meV. The inset shows schematically the composition of the Si(111) crystal with the 1/3 ML B layer displayed on an expanded scale.

Figure 2: HREELS measurements of surface hole-plasmon excitation on selectively B-doped Si(111). The incident electron energy is 6.1 eV at a 60° incident angle. The spectra correspond to increasing boron concentration in the near surface region following sucessive boron deposition and annealing cycles. The inset shows a plot of $(\Delta E)^2$ versus the B/Si Auger ratio.

Figure 3: HREELS measurement from a well-ordered Si(111)-B surface as a function of incident energy, E_0, at 100 K. The dashed line marks the frequency of the B-Si vibrational mode, ν(B-Si).

Figure 4: Comparison between theory and experimental HREELS measurement. The solid theoretical curve is based on the Thomas-Fermi model dielectric function, ε_{TF}, and dipole scattering theory. The best fit to the experimental spectrum is obtained with n_h=2.8x10^{19} cm^{-3} and a damping factor Γ= 74 meV, which corresponds a surface plasmon frequency ω_{sp}=102 meV and a loss peak position ω_{pp}=88 meV. The dashed curve is the k-integrated loss function Im[-1/(ε+1)]. A Gaussian function with 11 meV FWHM has been used to simulate the elastic peak.

Figure 5: Calculated energy loss spectra $I(\omega)$ as a function of E_0 based on the best-fit parameters discussed in the text. The solid curves are for a spectrometer acceptance angle ϑ_c=2.5°, the dashed ones for ϑ_c=3.0°.

Structure of Si(111)–B($\sqrt{3}$x$\sqrt{3}$)R30° Surface and HREELS Studies

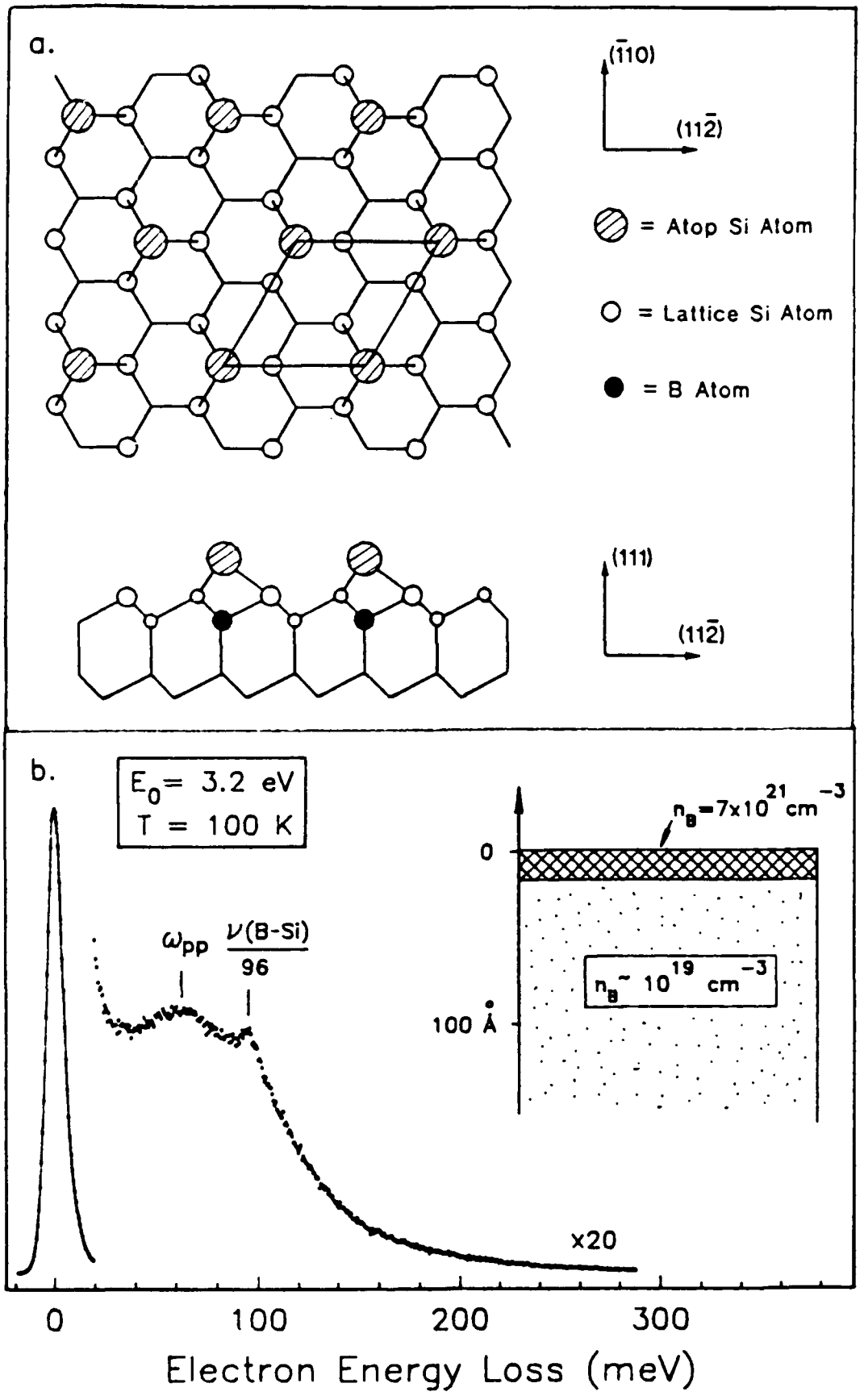

Chen, et al.

Figure 1

Surface Hole–plasmon Loss as a Function of Boron Concentration

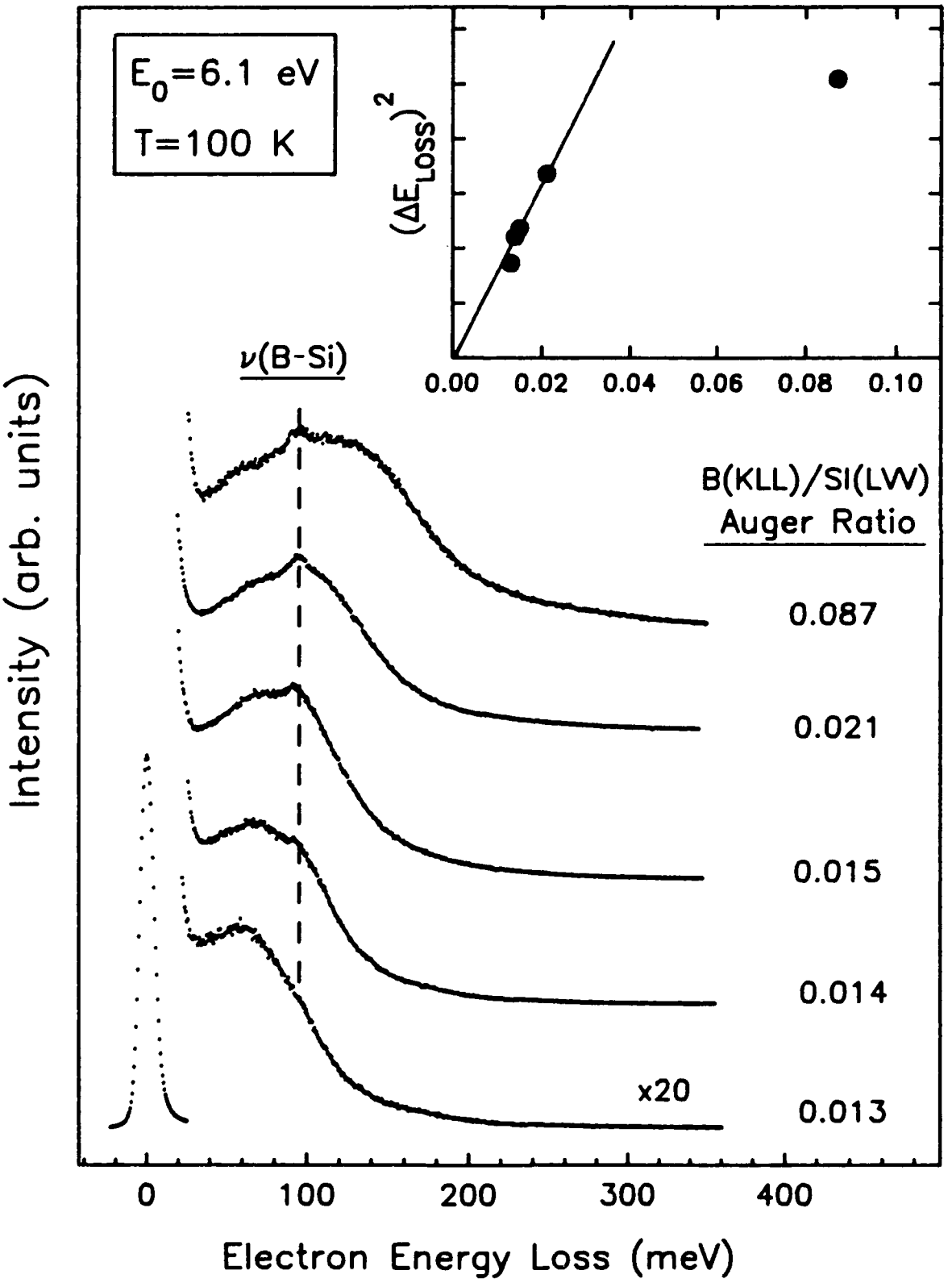

Chen, et al.

Figure 2

Surface Hole–Plasmon Loss as a Function of Incident Electron Energy

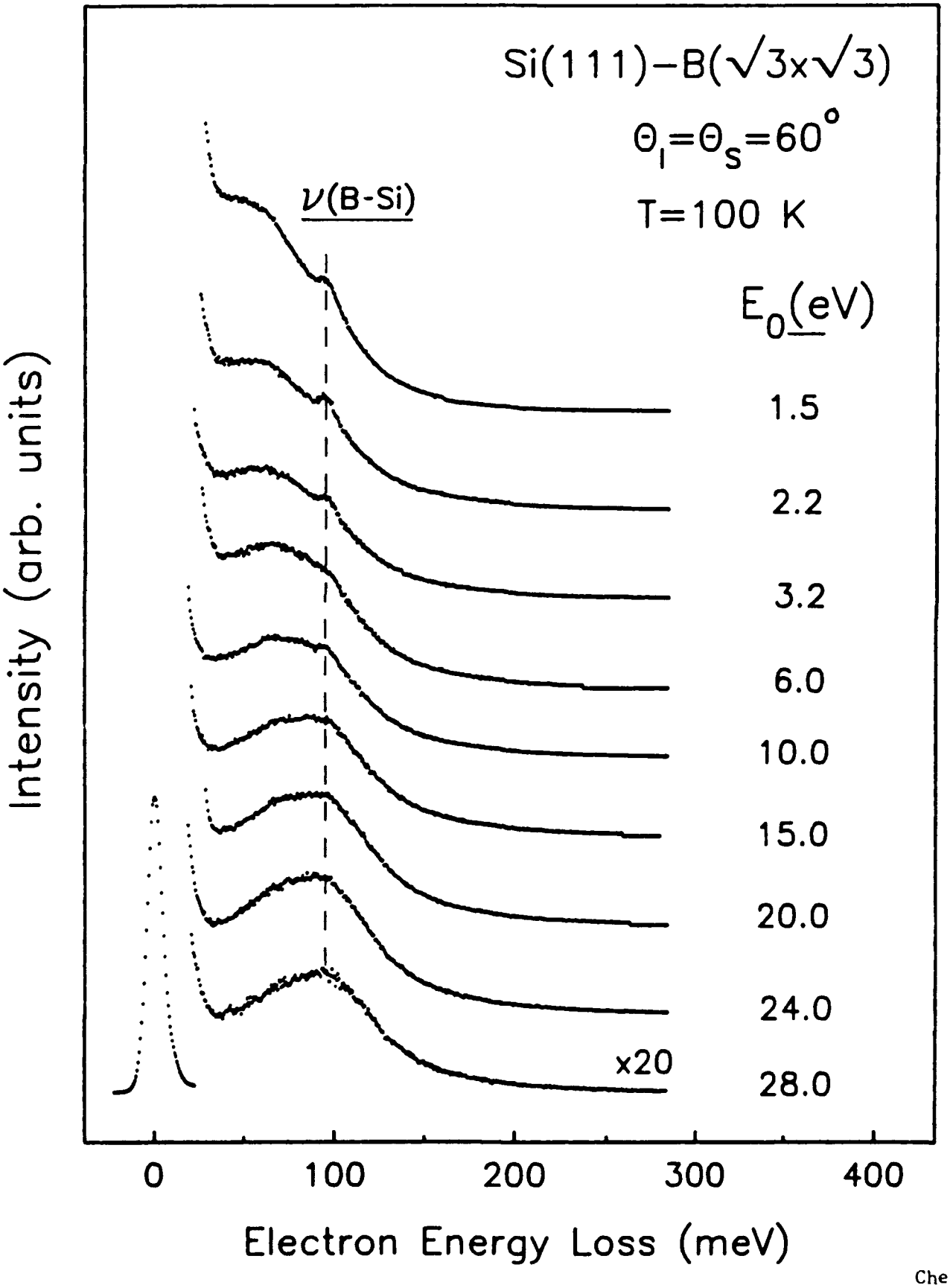

Chen, et al.

Figure 3

Comparison between Dipole Scattering Theory with Model Dielectric Function and HREELS Measurement on Si(111)–B

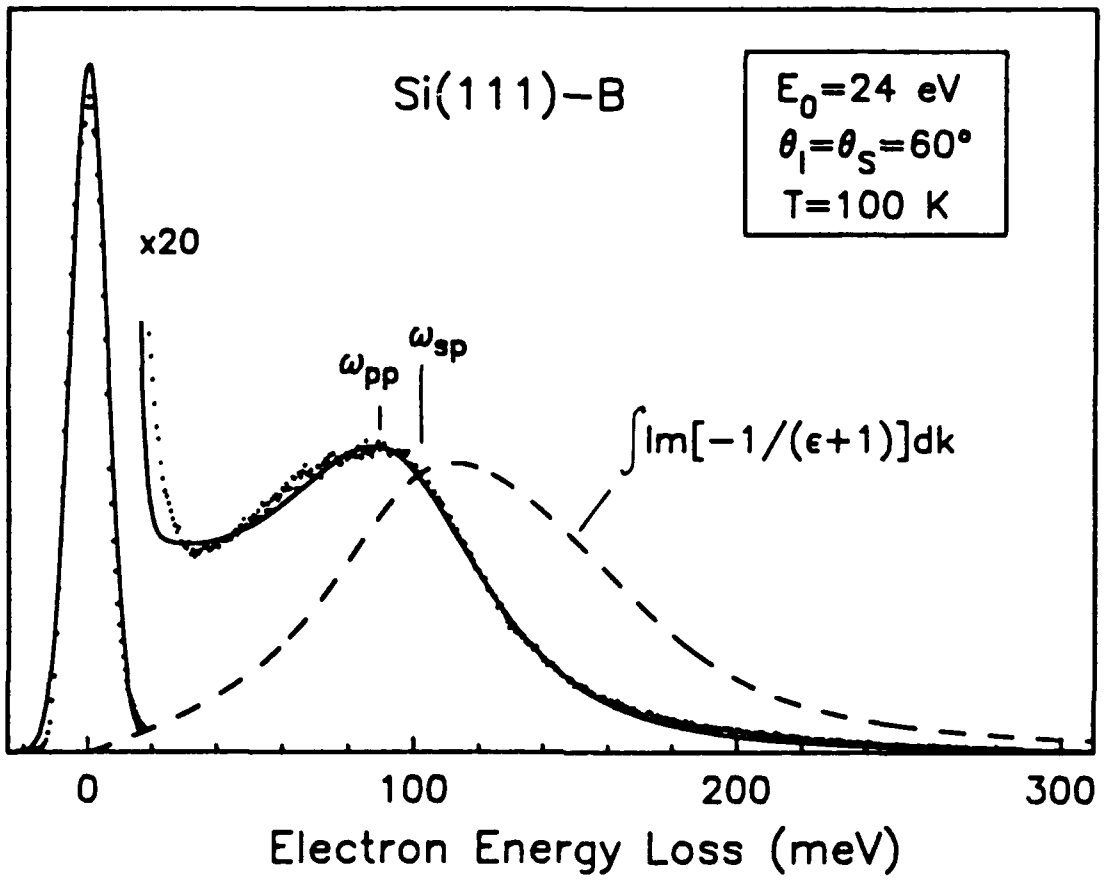

Chen, et al.
Figure 4

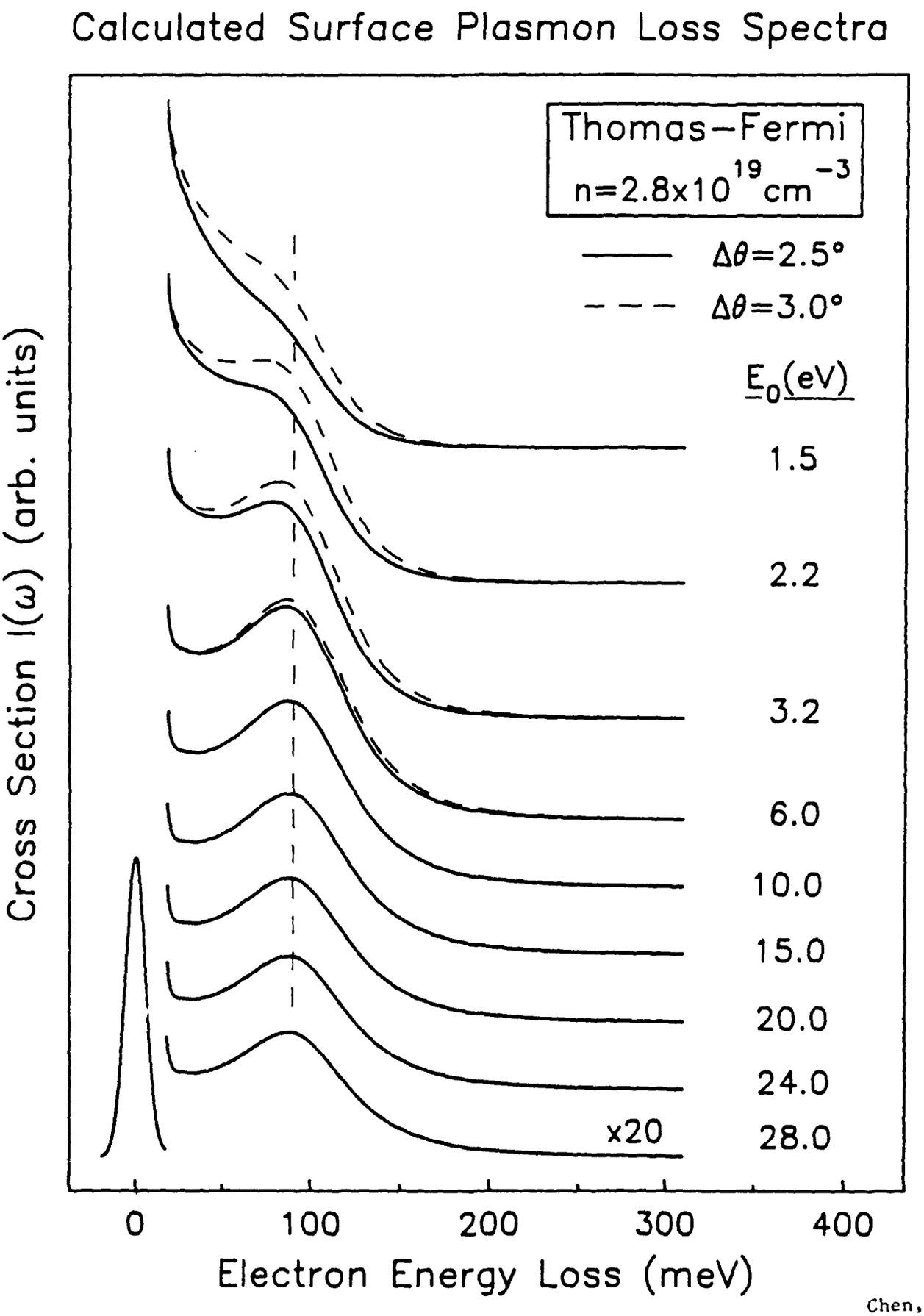

Chen, et al.

Figure 5

ALE Contractor Distribution List # Copies

D.T.I.C. 12
Bldg # 5, Cameron Station
Alexandria, VA 22314

Dr. Andrew Freedman 1
Aerodyne Research, Inc.
45 Manning Road
Billerica, MA 01821
Tel: (508) 663-9500
FAX: (508) 663-4918
e-mail: aerodyn@mitvma.mit.edu

Dr. Asif Kahn 1
APA Optics
2950 NE 84th Lane
Blaine, MN 55434
Tel: (612) 784-4995
FAX: (612) 784-2038
e-mail: 70702.2032@compuserve.com

Dr. Duncan Brown 1
Advanced Technology Materials, Inc
7 Commerce Drive
Danbury, CT 06810
Tel: (203) 794-1100
FAX: (203) 792-8040

Dr. Peter Norris 1
EMCORE Corp.
35 Elizabeth Ave.
Somerset, NJ 08873
Tel: (201) 271-9090

Prof. Joe Greene 1
Dept. of Materials Science and Engineering
University of Illinois
1101 W. Springfield Ave.
Urbana, IL 61801
Tel: (217) 333-0747

Dr. T. P. Smith 1
IBM T.J. Watson Research Center
P. O. Box 218, Route 134
Yorktown Heights, NY 10598
e-mail: trey@ibm.com

Prof. Robert F. Davis 1
N.C.S.U. Box 7907

Raleigh, NC 27695-7907
Tel: (919) 515-2377/3272
FAX: (919) 515-3419
e-mail: davis@mte.ncsu.edu

Prof. Salah Bedair 1
Department of Electrical Engineering
N.C.S.U.; Box
Raleigh, NC 27695
Tel: (919) 515-2336
e-mail: jll@@ecegrad.ncsu.edu

Max N. Yoder 1
ONR Code 1114
Arlington, VA 22217
Tel: (703) 696-4218
FAXes (703) 696-2611/3945/5383
e-mail: yoder@charm.isi.edu

Dr. A. M. Goodman 1
ONR, Code 1114
Arlington, VA 22217
Tel: (703) 696-4218
FAXes (703) 696-2611/3945/5383
e-mail: goodman@ocnr-hq.navy.mil

Dr. J. Pazik 1
ONR Code 1113
Arlington, VA 22217
Tel: (703) 696-4410
FAXes (703) 696-2611/3945/5383
e-mail: pazik@ocnr-hq.navy.mil
pazik%estd.decnet@ccf.nrl.navy.mil

Prof. J. T. Yates, Jr. 1
Dept. of Chemistry
Surface Science Ctr.
University of Pittsburgh
Pittsburgh, PA 15260
Tel: (412) 624-8320
FAX: (412) 624-8552
e-mail: yates@vms.cis.pitt.edu

Robert J. Markunas, R.A. Rudder 1
Research Triangle Institute; Box 12194
Research Triangle Park, NC 27709-2194
Tel: (919) 541-6153
FAX: (919) 541-6515
e-mail: rjmk@rti.rti.org

Professor Mark P. D'Evelyn 1
William Marsh Rice University
Dept. of Chemistry
P.O. Box 1892
Houston, TX 77251
Tel: (713) 527-8101, ext. 3468
FAX: (713) 285-5155
e-mail: mpdev@@langmuir.rice.edu

Dr. Howard K. Schmidt 1
Schmidt Instruments, Inc.
2476 Bolsover, Suite 234
Houston, TX 770054
Tel: (713) 529-9040

FAX: (713) 529-1147
e-mail: hksionwk@ricevml.rice.edu

Prof. A. F. Tasch 1
Dept. of Electrical Engr. & Computer Science
Engineering Science Bldg.
University of Texas at Austin
Austin, TX 78712
Tel:
FAX:
e-mail: tasch@roz.ece.utexas.edu

Prof. Charles Tu 1
Dept of Electrical & Computer Engr.
UCSD
LaJolla, CA
Tel: (619) 534-4687
FAX: (619) 534-2486
e-mail: cwt@celece.ucsd.edu

Prof. John E. Crowell 1
Department of Chemistry
University of California at San Diego
LaJolla, CA
Tel: (619) 534-5441
FAX: (619) 534-0058
email: jcrowell@ucsd.edu

Prof. P. Daniel Dapkus 1
University of Southern California
University Park
Los Angeles, CA 90089-1147
e-mail: dapkus@mizar.usc.edu
Tel: (213) 740-4414
FAX: (213) 740-8684

Unless you are a small business invoking your 2 year proprietory rights clause, you MUST state on the front page of your report: Approved for Public Release; distribution unlimited.